Int. Journal of Refractory Metals and Hard Materials 35 (2012) 10–16

Contents lists available at SciVerse ScienceDirect

Int. Journal of Refractory Metals and Hard Materials

journal homepage: www.elsevier.com/locate/IJRMHM

Erosion wear of CrN, TiN, CrAlN, and TiAlN PVD nitride coatings

Deng Jianxin *, Wu Fengfang, Lian Yunsong, Xing Youqiang, Li Shipeng

Department of Mechanical Engineering, Shandong University, Jinan 250061, Shandong Province, PR China

ARTICLE INFO

Article history:
Received 5 February 2012
Accepted 2 March 2012

Keywords:
Nitride coatings
PVD
Erosion wear
Wear mechanisms

ABSTRACT

Four nitride coatings (CrN, ZrN, CrAlN, and TiAlN) were deposited on YT15 cemented carbide by cathode arc-evaporation technique. Microstructural and fundamental properties of these nitride coatings were examined. Erosion wear tests were carried out, the erosion wear of these nitride coatings caused by abrasive particle impact was compared by determining the wear depth and the erosion rates of the coatings. The wear surface features were examined by scanning electron microscopy. Results showed that the coatings with Al (CrAlN and TiAlN) exhibited higher erosion wear resistance over those without Al (CrN and TiN). The H^3/E^2 of the coating seemed to play an important role with respect to its erosion wear in erosion tests. AlTiN and CrAlN coatings being with high H^3/E^2 exhibited lower erosion rates, while CrN coating with low H^3/E^2 showed higher erosion rates under the same test conditions. Analysis of eroded surface of the coatings demonstrated that the TiN and CrN coatings exhibited a typical brittle fracture induced removal process, while AlTiN and CrAlN coatings showed mainly micro cutting and cycle fatigue fracture of material removal mode.

1. Introduction

Surface coating is an effective method to improve the durability of the materials used in the aggressive environments. By selecting proper coating methods and coating materials, we may prolong the service life of the substrate material and increase the commercial value of the products. New coating deposition techniques developed over the last two decades offer a wide variety of possibilities to tailor surfaces with many different materials and structures. In particular, chemical vapour deposition (CVD) and physical vapour deposition (PVD) techniques have made it possible to deposit thin coatings a few micro-metre thick in a temperature range from high temperatures down to room temperature. Hard coatings are of interest in a number of technological fields due to their physical, chemical and mechanical properties. Coating materials such as TiN, TiC, CrN and more recently diamond, diamondlike carbon (DLC) and MoS_2 and their combinations as multi-layers have been used with great success [1–6]. Especially, hard nitride coatings are extensively used in many types of cutting operations, where they enhance tool life, improve surface finish and increase productivity [7–9].

Nitride based hard compound coatings prepared by various physical vapor deposition processes are finding increasing applications for nearly every demand. High hardness, excellent wear and corrosion resistance enable them significantly improve tool life. The first generation PVD nitride coatings featured TiN as the hard coating and were applied in interrupted cutting such as milling of steels. The superior performance of PVD TiN coated tools prompted their use in other machining applications, such as turning, as well as in industries as a wear-resistant or protective layer on the dies [10–13]. Afterwards various alloying elements have been added to improve the properties of the coatings. The addition of Al to form ternary thin films, e.g. TiAlN, is particularly attractive. TiAlN coatings have been developed as an alternative to TiN, because of their higher oxidation resistance, higher hardness and higher corrosion resistance. In addition, low thermal conductivity of TiAlN enables higher cutting speeds. The continued success of the PVD nitride coatings led to the commercial development of second and third generation PVD coatings which offer even higher machining productivity [14–19]. Some studies have proved that these nitride coatings have good mechanical properties [14,15], and excellent oxidation and wear resistance [16,17]. With respect to the erosion properties, several researchers [18–24] have studied the sand erosion performance of the coatings. Nevertheless, the knowledge about the comparatively erosion properties of these nitride coatings is poor.

In the present study, Four nitride coatings (CrN, ZrN, CrAlN, and TiAlN) were deposited on YT15 (WC + 15%TiC + 6%Co) cemented carbide by cathode arc-evaporation technique. Microstructural and fundamental properties of these nitride coatings were examined. Erosion wear tests were carried out with these nitride coatings. The wear surface features of were examined by scanning electron microscopy, and the wear mechanisms were investigated.

2. Experimental procedures

2.1. Preparation of PVD nitride coatings

The substrate material employed for this study was YT15 (WC + 15 wt.% TiC + 6 wt.% Co) cemented carbide. Data for hardness, flexural

* Corresponding author. Tel.: +86 0531 88392047.
E-mail address: jxdeng@sdu.edu.cn (J. Deng).

0263-4368/$ – see front matter © 2012 Elsevier Ltd. All rights reserved.
doi:10.1016/j.ijrmhm.2012.03.002

Table 1
Properties of the YT15 cemented carbide substrate.

Composition (wt.%)	Density (g/cm^3)	Hardness (GPa)	Flexural strength (MPa)	Fracture toughness ($MPa\ m^{1/2}$)	Thermal conductivity (W/(m K))	Thermal expansion coefficient (10^{-6}/K)
WC + 15% TiC + 6% Co	11.5	15.5	1130.0	12.0	33.47	6.51

Table 2
The PVD coating conditions.

Coating temperature (°C)	Total gas pressure (Pa)	Bias voltage (V)	Cathode current (A)	Coating time (min)	Source to substrate distance (mm)	Power (KW)
200	1.5	−40 to −150	60	60	200	2.5

strength, and fracture toughness of the YT15 cemented carbide are listed in Table 1. Before deposition the specimens were mirror-polished (1 μm diamonds) and ultrasonically cleaned in acetone and alcohol progressively, each for 5 min, and dried for approximately 20 min in a pre-vacuum dryer. Pure Ti, Cr targets and TiAl, AlCr composite targets with nitrogen gas (N_2) were introduced into the chamber as a reactive atmosphere to obtain all the coatings. The specimens were deposited at 200 °C, the DC-substrate bias voltage was in the range of −40 V to −150 V, Ar and N_2 flow were independently controlled using a mass-flow controller, the durations for depositing were 60 min. All the PVD coating conditions are listed in Table 2.

The phase compositions were examined by XRD (D/max-2400). The film thickness was measured by a surface profilometer (Wyko NT9300). In addition, to verify the obtained results, measurements of the coatings were made also on the cross-sectional view with scanning electron microscope. The hardness tests of coatings were made on the MH-6 hardness tester. Measurements were made at 0.2 N loads, eliminating influence of the substrate on the measurement results. Adhesion evaluation of the coatings was made using the scratch test on the MFT-3000 device, by moving the diamond penetrator along the examined specimen's surface with the gradually increasing load. The tests were made with the following parameters: radius of Rockwell diamond stylus 200 μm, load range 0–100 N, load increase rate 100 N/min, penetrator's travel speed 10 mm/min.

2.2. Erosion wear tests

Erosion wear tests were conducted with a dry blasting machine tool. The photo of this equipment is shown in Fig. 1. The impingement angle of the jet relative to the coating surface was 90°. The test piece was mounted at 20 mm distance from the end of the nozzle. The compressed air pressure was set at 0.5 MPa. The erodent abrasives used in this study were of silicon carbide (SiC) powders with 40–100 μm grain size. The SEM micrograph of the SiC powders is shown in Fig. 2. As these abrasives are more durable and create less dust than sand, and typically are reclaimed and reused. The wear mass loss of the coatings after the tests was too small to be resolved by weighing. Instead, the geometry of the eroded surface was measured with an optical profilometer (Wyko NT9300). At each test interval the distance between the original and the worn surfaces at the deepest position was measured and designated as the wear depth. The erosion rates (W) of the coatings are defined as the wear depth of the coating divided by the erosion time. Since the test parameters were kept constant, wear of the coatings should only depend on the nature of the coatings. The eroded surfaces of the nitride coatings were examined by scanning electron microscopy.

Fig. 1. Photo of the erosion test equipment.

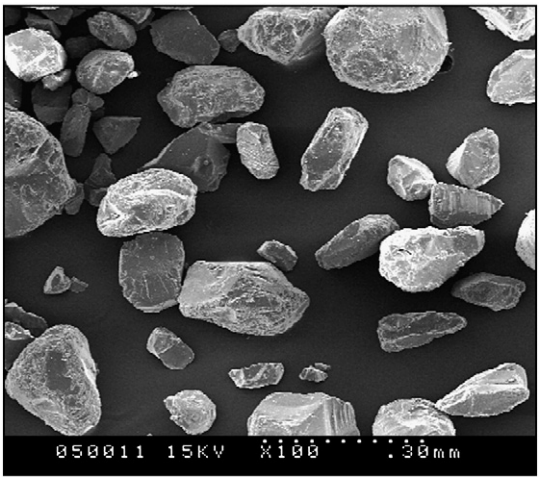

Fig. 2. SEM micrograph of the SiC abrasives used for erosion tests.

3. Results and discussion

3.1. Properties and microstructures of the nitride coatings

Hardness, critical load, and coating thickness of the investigated nitride coatings are presented in Table 3. It was revealed that the uncoated YT15 cemented carbide has a hardness of 15.5 GPa (see Table 1). Deposition of the PVD coatings onto the specimens causes the surface layer hardness increase. The hardness of TiAlN coating reaches 32.4 GPa, that is up to 100.0% more compared to that of YT15 substrate; while the hardness of CrN shows only a little increase (16.5 GPa) compared with that of the YT15 substrate. The critical load characterizing the adherence of the coating to the substrate was determined as the one corresponding to the acoustic emission (AE) increase signalling beginning of spalling of the coating in scratch test. It was found that the critical load of CrN, CrAlN, and TiAlN coatings is more than 80.0 N.

Table 3
Properties of the CrN, ZrN, CrAlN, and TiAlN nitride coatings.

Coatings	Elastic modulus (GPa)	Hardness (GPa)	Critical load (N)	Coating thickness (μm)
CrN	360	16.5	80.3	1.79
TiN	483	23.6	54.5	2.24
CrAlN	502	29.1	85.3	2.02
TiAlN	526	32.4	80.6	2.64

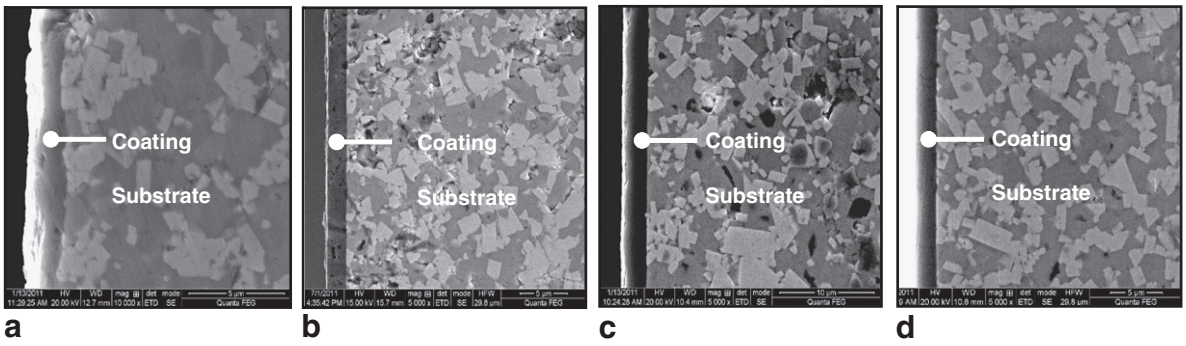

Fig. 3. SEM micrographs of the cross-sectional image of (a) CrN, (b) TiN, (c) CrAlN, and (d) TiAlN coatings.

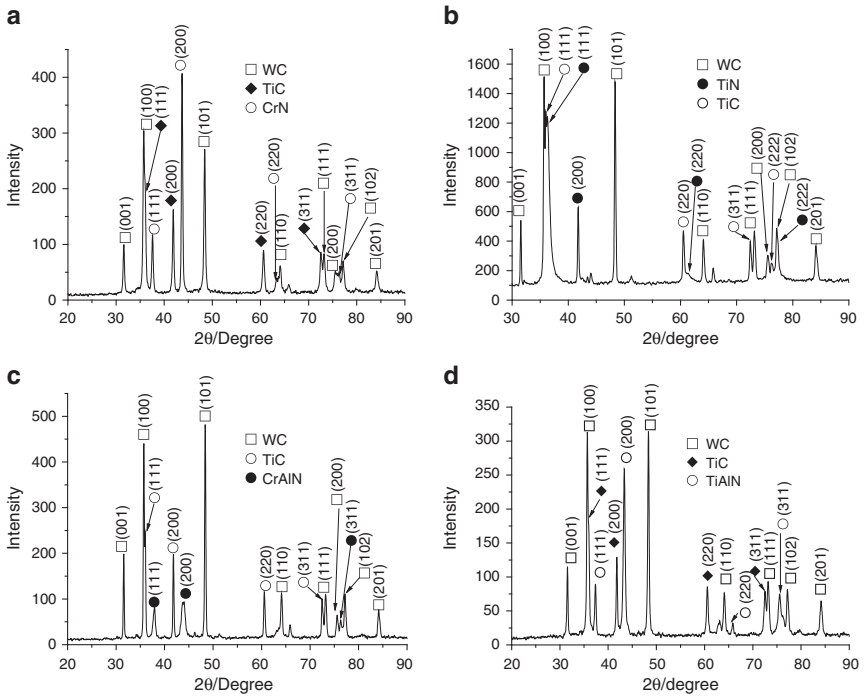

Fig. 4. X-ray diffraction analysis of (a) CrN, (b) TiN, (c) CrAlN, and (d) TiAlN coatings.

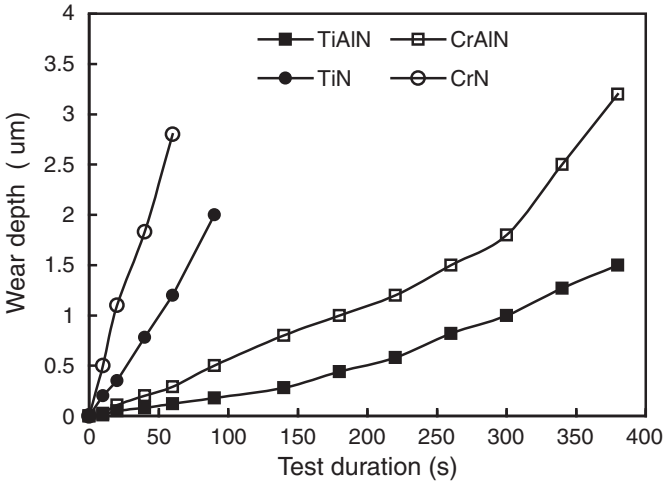

Fig. 5. Erosion wear depth of CrN, TiN, CrAlN, and TiAlN coatings as a function of test duration.

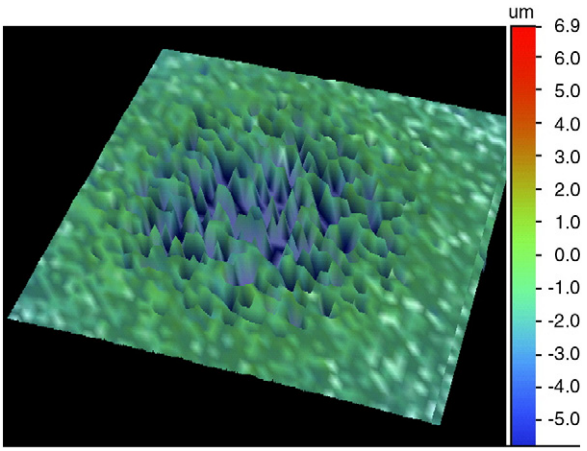

Fig. 6. Three-dimensional surface topography of the erosion scar of TiN coating after 60 s erosion operation.

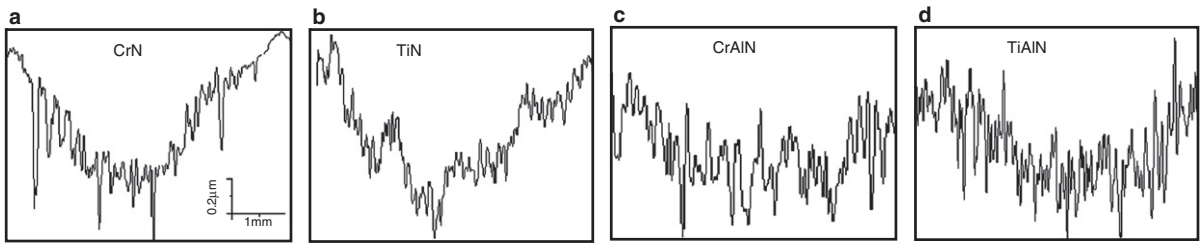

Fig. 7. Two-dimensional profiles of the wear tracks of (a) CrN, (b) TiN, (c) CrAlN, and (d) TiAlN coatings after 60 s erosion operation.

Fig. 3 shows the SEM micrographs of the cross-sectional image of the CrN, TiN, CrAlN, and TiAlN coatings. It shows a dense and fine grained coating structure, the coating thickness is in the range of 1.8 μm–3.0 μm. Fig. 4 illustrates the X-ray diffraction analysis of CrN, TiN, CrAlN, and TiAlN coatings.

3.2. Erosion wear behaviors of the nitride coatings

The wear depth is different for the nitride coatings depending on the erosion time. Fig. 5 shows the wear depth of CrN, TiN, CrAlN, and TiAlN coatings as a function of test duration. It is noted that the wear depth of the nitride coatings continuously increased with the operation time. Among all the coatings tested, the TiAlN coating showed the smallest wear depth under the same test conditions; while the CrN coating exhibited the highest wear depth. The time of coating penetration for CrN coating is about 40 s (see Fig. 5), since the wear depth reaches 1.8 μm after 40 s erosion operation (the coating thickness of CrN is 1.81 μm as can be seen in Table 3). While for TiAlN coating, the wear depth reaches only 1.5 μm after 380 s erosion operation, which is far less its coating thickness (2.64 μm). Therefore, the TiAlN coating was proved to have the highest erosion resistance over the other coatings.

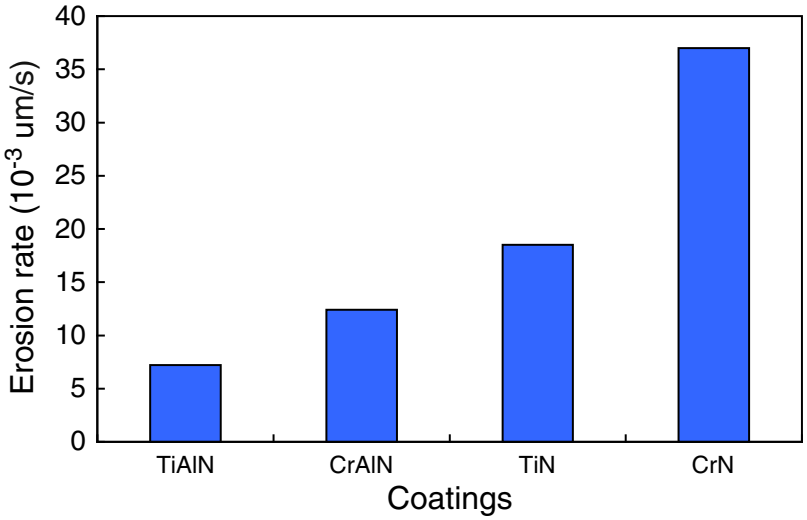

Fig. 8. Erosion rates of the CrN, TiN, CrAlN, and TiAlN coatings.

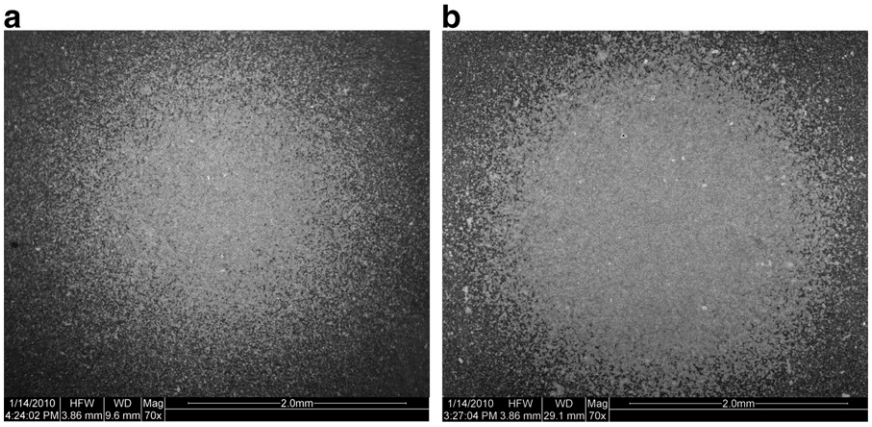

Fig. 9. SEM micrographs at lower magnification of the eroded surface of TiN coating after (a) 60 s and (b) 120 s erosion operation.

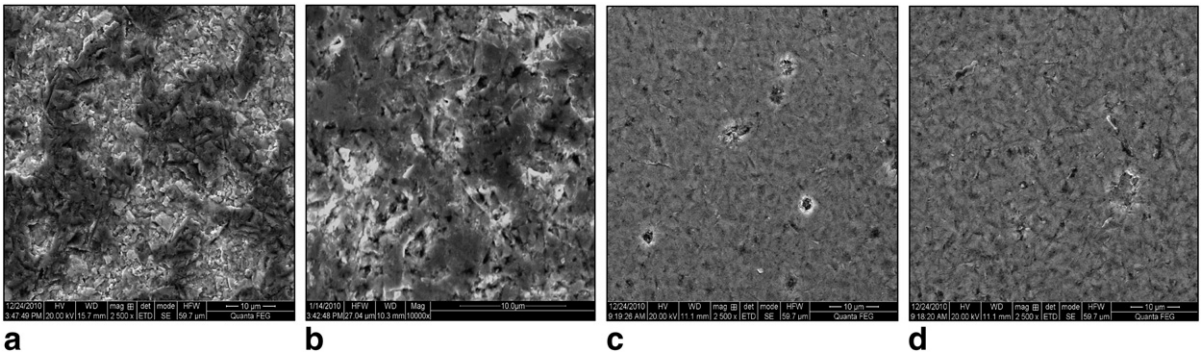

Fig. 10. SEM micrographs of the eroded surface of (a) CrN, (b) TiN, (c) CrAlN, and (d) TiAlN coatings after 60 s erosion operation.

Fig. 6 shows the three-dimensional surface topography of the erosion scar produced on TiN coating after 60 s erosion operation. It can be seen that the wear track of TiN coating shows a lot of small cavities on the eroded surface. Two-dimensional profiles of the wear tracks of CrN, TiN, CrAlN, and TiAlN coatings after 60 s erosion operation are shown in Fig. 7. The surface roughness (*Ra*) measured by profilometer of CrN, TiN, CrAlN, and TiAlN coatings after 60 s erosion operation is 1.78 μm, 1.42 μm, 0.52, and 0.41 μm respectively. The results also confirm that surface roughness of TiAlN coating is smaller than that of other coatings under the same test conditions.

Fig. 8 shows the erosion rates of CrN, TiN, CrAlN, and TiAlN coatings in erosion tests. The wear rate was found to decrease in the order TiAlN, CrAlN, TiN, CrN. The values of the wear rate are 37.0, 18.5, 12.4, and 7.2 for CrN, TiN, CrAlN, and TiAlN coatings respectively. The TiAlN coating exhibited the smallest wear rates; while the CrN coating the highest wear rates under the same test conditions.

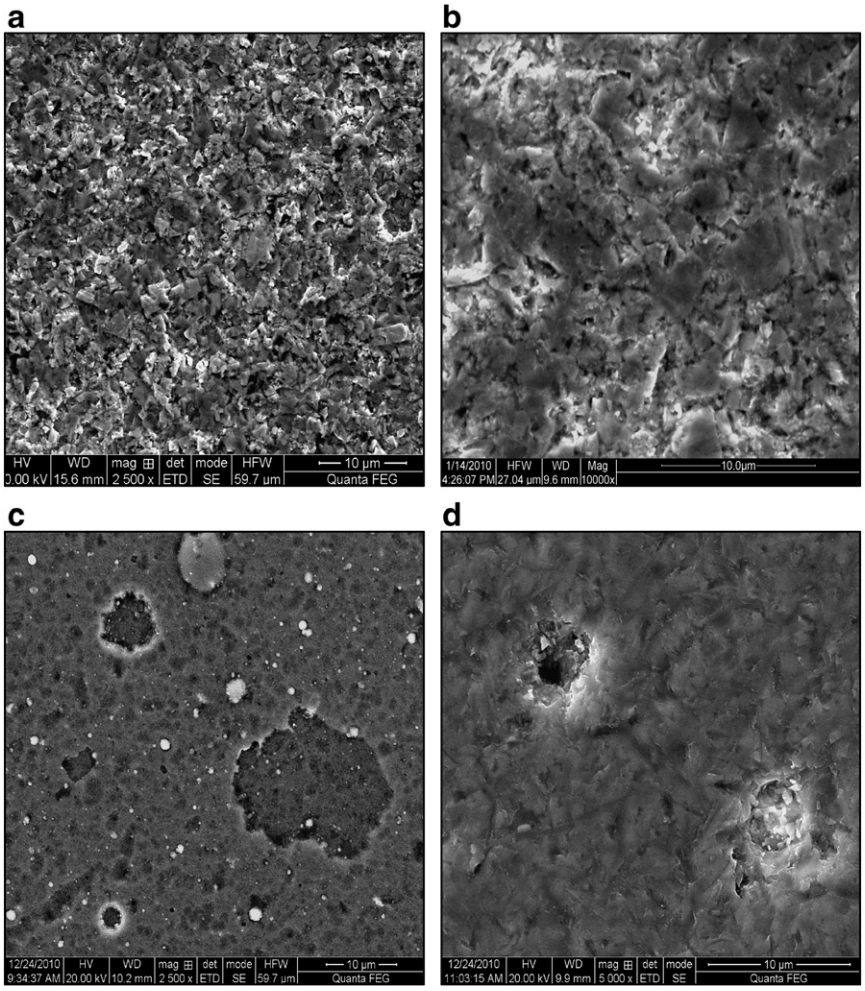

Fig. 11. SEM micrographs of the eroded surface of (a) CrN, (b) TiN, (c) CrAlN, and (d) TiAlN coatings after 120 s erosion operation.

3.3. Observation of worn surfaces

Fig. 9 shows representative SEM micrographs at lower magnification of the eroded surface of TiN coating after 60 s and 120 s erosion operation. It is noted that the erosion scar is about 3–4 mm in diameter. Closer examination at higher magnification of the wear tracks produced on the CrN, TiN, CrAlN, and TiAlN coatings are shown in Figs. 10 and 11. It is notable that the wear track of CrN coatings after 60 s erosion operation (Fig. 10(a)) revealed a rougher surface and partial coating removal. There were numerous pits on the eroded surfaces. Delamination and brittle fracture of the coating were observed, and the coating damages reached the YT15 substrate in some area of the wear track. The probability of finding such features on the eroded CrN coating is significantly greater. For TiN coating, a relatively smooth surface was produced and the substrate slightly appeared on the whole worn surface, insignificant traces of deep plowing grooves and micro chipping of small segments were revealed (Fig. 10(b)). While the wear track of CrAlN and TiAlN coatings after 60 s erosion operation showed a very smooth topography (Fig. 10(c) and (d)), and the initial exposure of the substrate was more local.

The coatings were worn gradually with the erosion time, and eventually the substrate was exposed and eroded. After 120 s erosion operation, the CrN coating was worn out completely, and the erosion wear was occurred on the YT15 cemented carbide substrate (Fig. 11(a)). Inspection of the wear tracks of CrAlN and TiAlN coatings after 120 s erosion operation revealed small delamination of the coating from the substrate (Fig. 11(c) (d)). The initial coating failure may also be accelerated by the presence of defects such as, for example, the local protuberances. Surface roughness is hardly being avoided because of droplets that are characteristic to PVD process. Cracking

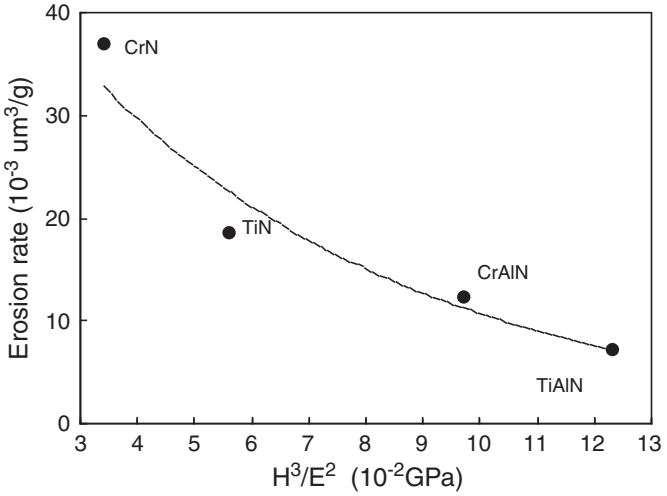

Fig. 13. Interdependence of H^3/E^2 and erosion rate of CrN, TiN, CrAlN, and TiAlN coatings.

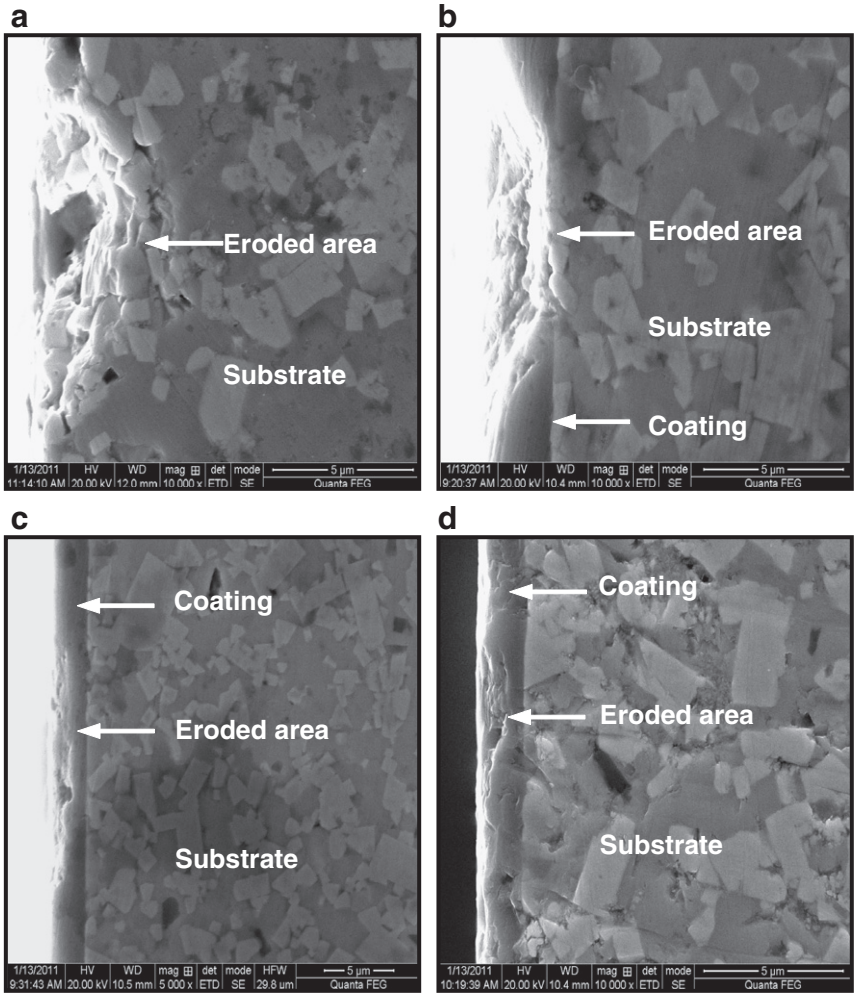

Fig. 12. The cross-sectional images of the eroded wear track of (a) CrN, (b) TiN, (c) CrAlN, and (d) TiAlN coatings after 120 s erosion operation.

and removal of the partial coating, all results in redistribution of the contact pressures and overstressing around the damaged areas that facilitates the further coating damage. After reaching of the critical size under repetitive impacts, the large chip may remove from the surface. It is concluded that the CrAlN and TiAlN coatings is removed in the form of small fragments due to repeated attacks from the small eroding particles.

The eroded coatings were cut after operation in vertical directions for failure analysis. Fig. 12 shows the cross-sectional images of the eroded wear track of CrN, TiN, CrAlN, and TiAlN coatings after 120 s erosion operation. It appears that the damages of CrN and TiN coatings have reached the YT15 substrate in the eroded area.

3.4. Discussion

In the erosion wear tests, fine particles are accelerated and are directed towards coating surfaces. As the particles impact the coating surface, they cause a small fracture, and the coating is removed primarily by repeated impact of the abrasive particles. Several studies [25–29] have been shown that impact of brittle materials by hard particles is generally thought to result from elastic/plastic fracture. This type of fracture is characterized firstly by plastic deformation of the contact area between the impacting particle and the material surface, with subsurface lateral cracks propagating outward from the base of the contact zone on the planes nearly parallel to the surface, and with median cracks propagating from the contact zone normal to the surface. The interaction of lateral and radial cracks is considered to result in material removal. Analysis of erosion of brittle materials typically recognizes two models of material removal: a ductile plowing type of material removal, and a fracture induced removal process. In the class of hard coatings presently being considered, both processes may occur, depending on the specific stress state. The high hardness of the coating is only one parameter which ensures scratch and abrasion resistance. The coatings must be highly resistant also to plastic deformation during contact events. The resistance of coating to plastic deformation can be controlled by the film hardness H and its elastic modulus E. The ratio H^3/E^2 is a parameter which controls the resistance of materials to plastic deformation [30,31]. Fig. 13 shows the interdependence of H^3/E^2 and erosion rate of the coatings. It is indicated that the H^3/E^2 of the coating material had an important influence on its erosion rate. The TiAlN coating is characterized by high resistance to plastic deformation (H^3/E^2) and lower erosion rate, while the coatings with relative low H^3/E^2 showed higher erosion rate.

4. Conclusions

Four nitride coatings (CrN, ZrN, CrAlN, and TiAlN) were deposited on YT15cemented carbide by cathode arc-evaporation technique. Erosion wear tests were carried out with these coatings. The following conclusions were obtained:

1. The coatings with Al (CrAlN and TiAlN) exhibited higher erosion wear resistance over those without Al (CrN and TiN).
2. The H^3/E^2 of the coating seemed to play an important role with respect to its erosion wear in erosion tests. The AlTiN coating being with high H^3/E^2 exhibited lower erosion rates, while CrN coating with low H^3/E^2 showed higher erosion rates under the same test conditions.
3. Analysis of eroded surface of the coatings demonstrated that TiN and CrN coatings exhibited a typical brittle fracture induced removal process which experienced solid particle erosion damage involving both delamination and brittle fracture; While AlTiN and CrAlN coatings experienced significantly less erosion damage than CrN and TiN coatings, and showed mainly micro cutting and cycle fatigue fracture of material removal mode.

Acknowledgement

This work is supported by “The National Natural Science Foundation of China (51075237)”, “The Taishan Scholar Program of Shandong Province”, “The Outstanding Young Scholar Science Foundation of Shandong (JQ200917)”, “The Independent Innovation Foundation of Shandong University (2011JC001)”, and “The Specialized Research Fund for Doctoral Program of Higher Education (20110131130002)”.

References

[1] Prengel HG, Pfouts WR, Santhanam AT. State of the art in hard coatings for carbide cutting tools. Surf Coat Technol 1998;102:183–90.
[2] Klocke F, Krieg T. Coated too1s for metal cutting features and applications. Ann CIRP 1999;48:515–25.
[3] Kalss W, Reiter A, Derflinger V, Gey C, Endrino JL. Modern coatings in high performance cutting applications. Int J Refract Metals Hard Mater 2006;24:399–404.
[4] Ducros C, Benevent V, Sanchette F. Deposition, characterization and machining performance of multilayer PVD coatings on cemented carbide cutting tools. Surf Coat Technol 2003;163–164:681–8.
[5] Uhlmann E, Lachmund U, Brücher M. Wear behavior of HFCVD-diamond coated carbide and ceramic tools. Surf Coat Technol 2000;131:395–9.
[6] Renevier NM, Lobiondo N, Fox VC, Teer DG, Hampshire J. Performance of MoS_2/-metal composite coatings used for dry machining and other industrial applications. Surf Coat Technol 2000;123:84–91.
[7] Ezugwu EO, Okeke CI. Tool life and wear mechanisms of TiN coated tools in an intermittent cutting operation. J Mater Proc Technol 2001;116:10–5.
[8] Soković M, Bahor M. On the inter-relationships of some machinability parameters in finish machining with cermet TiN (PVD) coated tools. J Mater Proc Technol 1998;78:163–70.
[9] Deng JX, Liu JH, Zhao JL, Song WL, Niu M. Friction and wear behaviors of the PVD ZrN coated carbide in sliding wear tests and in machining processes. Wear 2008;264:298–307.
[10] Fenske GR. Nitride and carbide coatings for high speed steel cutting tools. Trib Trans 1989;32:339–45.
[11] Sahin Y, Sur G. The effect of Al_2O_3, TiN and Ti (C, N) based CVD coatings on tool wear in machining metal matrix composites. Surf Coat Technol 2004;179:349–55.
[12] Jindal PC, Santhanam AT, Schleinkofer U, Shuster AF. Performance of PVD TiN, TiCN, and TiAlN coated cemented carbide tools in turning. Int J Refract Metals Hard Mater 1999;17:163–70.
[13] Harris SG, Doyle ED, Vlasveld AC. Influence of chromium content on the dry machining performance of cathodic arc evaporated TiAlN coatings. Wear 2003;254:185–94.
[14] Horling A, Hultman L, Oden M, Sjolen J, Karlsson L. Mechanical properties and machining performance of $Ti_{1-x}Al_xN$ coated cutting tools. Surf Coat Technol 2005;191:384–92.
[15] Barshilia HC, Prakash MS, Jain A, Rajam KS. Structure, hardness and thermal stability of TiAlN and nanolayered TiAlN/CrN multilayer films. Vacuum 2005;77:169–79.
[16] Panjan P, Navinsek B, Cekada M, Zalar A. Oxidation behaviour of TiAlN coatings sputtered at low temperature. Vacuum 1999;53:127–33.
[17] Kim CW, Kim KH. Anti-oxidation properties of TiAlN film prepared by plasma-assisted chemical vapor deposition and roles of Al. Thin Solid Films 1997;307:113–9.
[18] Spain E, Avelar-Batista JC, Letch M, Housden J, Lerga B. Characterisation and applications of CrAlN coatings. Surf Coat Technol 2005;200:1507–13.
[19] Wang L, Nie X, Housden J, Spain E, Jiang JC, Meletis EI, et al. Material transfer phenomena and failure mechanisms of a nanostructured CrAlN coating in laboratory wear tests and an industrial punch tool application. Surf Coat Technol 2008;203:816–21.
[20] Wood RJK. The sand erosion performance of coatings. Mater Des 1999;20:179–91.
[21] Iwai Y, Miyajima T, Honda T, Matsubara T, Kanda K. Evaluation of erosive wear resistance of TiN coatings by a slurry jet impact test. Wear 2006;261:112–8.
[22] Mann BS. High-energy particle impact wear resistance of hard coatings and their application in hydroturbines. Wear 2000;237:140–6.
[23] Antonov M, Hussainova L, Sergejev F, Kulu P, Gregor A. Assessment of gradient and nanogradient PVD coatings behaviour under erosive, abrasive and impact wear conditions. Wear 2009;267:898–906.
[24] Iwai Y, Miyajima T, Mizuno A, Honda T, Itou T, Hogmark S. Micro-slurry-jet erosion (MSE) testing of CVD TiC/TiN and TiC coatings. Wear 2009;267:264–9.
[25] Lawn BR, Evans AG, Marshall DB. Elastic/plastic indentation damage in ceramics: the median/radial crack system. J Am Ceram Soc 1980;63:574–81.
[26] Buijs M. Erosion of glass as modeled by indentation theory. J Am Ceram Soc 1994;77:1678–82.
[27] Deng JX. Erosion wear of boron carbide nozzles by abrasive air-jets. Mater Sci Eng A 2005;408:227–33.
[28] Marshall DB, Lawn BR, Evans AG. Elastic/plastic indentation damage in ceramics: the lateral crack system. J Am Ceram Soc 1982;65:561–6.
[29] Wood RJK, Wheeler DW, Lejeau DC. Sand erosion performance of CVD boron carbide coated tungsten carbide. Wear 1999;233–235:134–50.
[30] Musil J. Hard and superhard nanocomposite coatings. Surf Coat Technol 2000;125:322–30.
[31] Shtansky DV, Kiryukhantsev-Korneev PhV, Bashkova IA, Sheveiko AN, Levashov EA. Multicomponent nanostructured films for various tribological applications. Int J Refract Metals Hard Mater 2010;28:32–9.